Scientific Research Publishing

Journal of Power and Energy Engineering, 2024, 12, 1-33
https://www.scirp.org/journal/jpee
ISSN Online: 2327-5901
ISSN Print: 2327-588X

Inclined Window Solar Box Cooker with One External Reflector Designed for the Mediterranean Latitudes

Victor J. Law[1*], James F. Lalor[2], Denis P. Dowling[1]

[1]School of Mechanical and Materials Engineering, University College Dublin, Dublin, Ireland
[2]School of Mechanical Engineering, Technological University Dublin, Dublin, Ireland
Email: *viclaw66@gmail.com

How to cite this paper: Law, V.J., Lalor, J.F. and Dowling, D.P. (2024) Inclined Window Solar Box Cooker with One External Reflector Designed for the Mediterranean Latitudes. *Journal of Power and Energy Engineering*, **12**, 1-33.
https://doi.org/10.4236/jpee.2024.1211001

Received: October 3, 2024
Accepted: November 10, 2024
Published: November 13, 2024

Abstract

Off-grid solar cooking in the developed and developing regions of the world is becoming one response to climate change that causes wood-fuel shortages and an increase in cost of coal, gas, and electricity production and their transportation. This paper examines a series unloaded temperature and loaded (food) performance metrics for an inclined window solar box cooker (SBC) designed for Mediterranean latitudes (35.31˚N, 24.31˚E). Solar radiation analysis using two different computer software platforms (SunCalc and Autodesk Revit® with insight plug-in software) is used to date and time-stamp the solar box cooker solar input power. Performed sensible heat tests demonstrate that the solar cooker can reach unloaded internal temperatures of 120˚C at a solar irradiance of 192 W, and a first figure of merit of 0.08 to 0.105. Food cooking metrics is performed on: whole eggs-without water, and the following with water; White medium-grain rice, rice pudding, pastitsio #2 pasta and Brown small lentils. The analytical metrics reveals that their required cooking power is 13 to 53 W; cooking energy of 94 to 210 kJ and energy density is 0.2 to 0.6 $kJ \cdot g^{-1}$. Using day and time-stamped computed solar input power the food cooking power efficiency varies between 6% to 8.9% for three whole eggs-without water, and 16% to 35.5% for rice, pasta, and lentils cooked in water. For water-stressed communities in traditional desert and emerging drought regions a mass-based wastewater/product metrics is used to help drive the water efficiency of the solar cooking process.

Keywords

Solar Radiation, Solar Box Cooker, Food Cooking Metrics

1. Introduction

For more than two millennia, solar energy has been employed for drying, preserving, and cooking cereals, fruit, fish, and meat. In recent times the scientist and mountaineer Horace Bénédict de Saussure (1767), Sir John Herschel (1800) and others have harnessed the greenhouse effect to raise the temperature within a wooden box topped with layers of glass, here termed solar box cooker (SBC) for the slow-cooking of food-stuff at temperatures above 100˚C [1]. Notably de Saussure named his device a "*Heliothermometre*". Modern SBC fitted with external reflectors can reach unloaded internal temperatures of 110˚C to 140˚C; and once the window aperture is closed the temperatures falls to ambient temperature within a few hours, depending the degree of insulation employed. These temperature profiles make the SBC suitable for pasteurization of naturally contaminated water typically 62.8˚C for at least one hour 30 [2], the slow-cooking of food-stuff as well as keeping cooked food warm. The non-cardboard constructed SBC tends to be heavy (8 to 10 kg) and size of a microwave oven, or air fryer, and requires, at the very least, manual tracking of the Sun's apparent movement through the sky due to the earth's rotation on its axis. Additionally, the SBC offers significant health advantages over traditional open-fire cooking as there is minimal impact from wind-blown sand, dirt and other contaminates, it preserves many food micronutrients and vitamins due to low cooking temperatures, there is significantly reduced potential for burn injuries, and it also helps in keeping food warm during off-sunshine hours. Other advantages include easy handling, operating, and maintaining the oven over its projected lifespan.

Over the years, the focus of SBC development has shifted from cooking meals in a solar-rich, fossil fuel-poor regions (deserts etc.,) to other geographic locations where there is increasing interest in the low environmental impact yet economic cooking technology. Coupled with the increased frequency and scale of forest wildfires in the Americas and Europe that result in a reduction the amount of wood for open fire cooking and the pollution of local water resources [3] solar energy cooking is now becoming a viable alternative energy source for low-income families in the developing world [4] [5] and also enjoys great interests in off-grid communities in the developed world [6]. In equatorial regions between the tropic of Cancer (latitude +23.5 degrees) and the tropic of Capricorn (latitude −23.5 degree) there is free and abundant solar energy directly overhead twice a year, making it an obvious choice as the cooking energy source. In these equatorial regions studies have shown that SBC can provide a family meal all year round as long as the window aperture points to zenith (perpendicular to the horizontal) with the Sun tracking north to south and vise-versa over the course of the year [7]-[21]. Notable variations from this body of work include Adetifa and Aremu (2016) [22] who developed a top and bottom double exposure SBC, Folaranmi (2013) *et al.* [23] who used a window tilt angle set to the local latitude of 10 degrees in Nigeria. Soro *et al.* (2020) [24] has successful cooked food using a 65 degrees tilted window in the Côte d'Ivoire in unfavorable climatic conditions. Milikias

(2022) [25] and (2023) [26] used a window tilt angle of 23 degrees in Ethiopia. A tillable SBC located in Sana'a, Yemen has also been reported [27].

As we move away from the Torrid Zone near the equator, into either of the Earths temperate zones where the Sun is never overhead but progressively at slanting angles for shorter daylight hours and reduced number of sunny days for solar cooking is more of a challenge. For this reason the following references are characterized by climate zone rather than chronological to better reflect the SBC adaptations to these climates zones.

For regions/countries with latitudes between +24 and +29 degrees some of relevant studies are listed here. In Mexico, Terries *et al.* (2014) [28] and Terries *et al.* (2022) [29] investigated the use of augmented internal reflectors. In India Koshti, Dev, Bharti and Narayan (2023) [30] compared a SBC window zero title angle with their latitude title angle of 25 degrees. Kesarwani, Rai and Sachann (2015) [31] and Srivastava and Rai [32] studied the incorporation of high surface metal fines to cooking vessel to improve heat transfer efficiency. In Pakistan, Zafa *et al.* (2018) [33] introduced an L-shape SBC, and, Rizvi, Uzair and Siddiqul (2023) [34] used the SBC as a thermal storage box for serving cooked food in off-sunshine periods. Mullick, Kandpal and Saxena (1987) [35] were one of the first research teams to propose a standard test procedure for performance evaluation and standardization of the SBC. Sethi, Sumathy and Pal (2013) [36] developed a mathematical relationship between to compute optimum inclination angle of booster mirror for horizontally placed cooker. Ponnia, Singh, Santra and Jain (2019) [37] investigated how the figure of merit can be increased using high insulation materials and wall thickness, while Nahar (2023) [38] employed engine oil as an energy storage medium within a solar hot box cooker (SHBC). Finally in Malaysia, Kalidasan *et al.* (2023) [39] experimented with different shaped metal fines attached to the cooking vessel, in order to improve the cooking power and heat transfer efficiency of SBC.

In the southern temperate zone (−22 to −30 degrees latitude) Kunene, Mhazo, Mukabw and Masarirambi (2015) [40] made a comparison study between a solar Coolkit cooker with their home made SBC in Swaziland, whilst Mawire *et al.* (2020) [41] in South Africa and Namibia, used a *Wonderbag*' to extend the cooking of partially solar cooked food into the off-sunshine period without the need for additional heat.

For temperate regions and countries between +29 to +41 degrees (California, the Mediterranean Sea, and countries further East; Jordon, Iraq, Pakistan, and northern India) there is increase interest in the use of SBC for pasteurization and cooking. For example, Ciochetti and Metcalf used the Kerr-Cole Eco-Cooker for solar heat pasteurization of naturally contaminated water [2], In Algeria, Benbaha *et al.* (2023) [42] developed a mathematical thermal model for complex SBC with a tilted window, whilst Maammeur *et al.* (2024) [43] proposed the idea of a volume figure of merit for SBC with a titled window. More recently Belatrache *et al.* (2024) [44] investigated the thermal performance of a SHBC that is augmented with three

external reflectors and two wings (where the wings connect the three reflectors at their two Connors). In Portugal, Collares-Pereiraa, Cavacoa and Tavaresa (2018) [45] proposed a figure of merit based on the solar collector area/absorber plate ratio. In Türkiye Arabacigil, Yuksel and Avci (2015) [46] investigated SBC internal and external reflectors surfaces, followed by Cuce, Kolayl, and Cuce (2019) [47] claimed the first Green Chemistry product (propolis resinous mixture made from beewax) as a heat] storage medium. In Jordan, Qandil, Al-Younis, Saleh, and Hasson (2018) [48] reported on a comparative study of single, and double-glazed window performance of a SBC. Kadhid and Askar (2018) [49] and Ibrahim, Kadhim and Ali further developed thermal models for a SBC with window-tilt angle of 35 degree, in Baghdad, Iraq [50], and Kumar *et al.* (2022) [51] and Kumar *et al.* (2023) [52] investigated the application of phase change materials in both a SBC and SHBC, respectively.

Collectively these temperate zone studies demonstrate the need for the SBC window to be tilted (or inclined), to face towards the Sun. Moreover, to keep SBC batch production costs to a minimum the window is generally tilted to local geographical latitude. Taking the Crete city of Heraklio, as an example, the tilt angles with a southern orientation are typically between 30 [53] and 35.3 degrees [54]. It is worth noting that a number of SBC geometries have been reported with two angle positions that can be used, one optimized for low sun angle during winter months and the second angle more suited high sun angles in the summer months [5] [55]. To keep solar cooking times to a minimum the SBC is aligned to the Sun's geographic azimuth position (*i.e.* compass bearing) typically every 30 minutes (in northern hemisphere where the Sun moves westerly at a rate of 15 degrees per hour). In addition the external reflector zenith angle (ϕ_z) needs to be adjusted to Sun's declination ($\delta_\odot$) to maximize the amount of solar radiation directed into the absorber plate (cooking vessel) within the SBC. Thus $\delta_\odot$ and the external reflector act as a coupled system that has two-degrees of freedom; the Sun has a predictable position within the sky and the other is an operator controlled response to the prediction. However, this operation is generally glossed over in the references cited above. Indeed this coupled system is the inspiration of many automatic sun trackers [56]. For solar cooking the prediction of $\delta_\odot$ is generally based on the assumption that the earth's orbit is a perfect circle and 360 degrees can be dived into 365 days, an estimation of $\delta_\odot$ can be found using Equation (1) [57].

$$\delta_\odot = -23.5\sin\left[\frac{360}{365}\times\left(d+10\right)\right] \tag{1}$$

where d is the day of the year with January 1st = day 1, and +10 comes from the fact that the winter solstice (December 21st - 22nd) occurs before the start of the year. This equation provides a positional error of 2 degrees or 4 times the Sun's arc diameter which is acceptable for solar cooking purposes. A variation of this equation may be found in [10] [15] [23] [54].

The main purpose of the SBC is the for pasteurization of naturally contaminated water and to cook food, however the number publications in the above body

works describing the cooking of food is twelve out of fifty four, or some 20.3%. Moreover, the publications relating to cooking of food use different SBC types, cooking vessels, geographical location at different times of year that created a wide range of solar heating conditions.

The overall objective of this study is:

1) To describe the design, construction and build cost of a SBC fitted with a inclined double-glazed window and one single external reflector that is suitable for cooking a two person meal at a geographical location (35.31˚N, 24.31˚E at an altitude of 119 m) on the island of Crete, Eastern Mediterranean. This simple SBC design differs from the SHBC in that it has no additional thermal storage material or phase change martial [15] [34] [37] [38] [44] [46] [47] [50]-[52], nor does it have complex integrated Fresnel reflectors or vacuum tubes [42] [56].

2) Use SunCalc open-source software (https://www.suncalc.org) and Autodesk Revit® building information modeling (BIM) to compute the SBC solar input power on a given date, time and location.

3) Perform SBC sensible heat tests under variable and fixed external reflector ϕ_z position for optimum alignment to the Sun's geographical azimuth position: followed by calorimetric analysis.

4) With the SBC in the retained-heat mode and water loaded conditions to simulate cooked food safe warming times.

5) Using the SBC and one cooking vessel, undertake comparative solar cooking experiments of common household meals (eggs, white medium-grain rice, rice pudding, pastitsio #2 pasta, and Brown lentils) between 28.7.2024 and 19.8.2024 with a solar irradiance of 1010 ± 15 $W \cdot m^2$. By standardizing the major experimental variables a meaningful estimation of the food cooking power, process (cooking) energy budget (W multiplied by cooking time (s)), and energy density (process energy budget divided by mass of the load ($J \cdot g^{-1}$) is obtained. Finally, use the estimated input power to validate and the estimated thermal power efficiency solar cooking of foodstuff.

6) Sustainable development through the use of free solar energy and the reduction of valuable water resources is a grand challenge of chemistry and chemical engineering for the foreseeable future [58]. Here mass-based Environmental-Factor as defined here as wastewater/product is applied to SBC common household meals recipes.

2. Eastern Mediterranean SBC Design, Construction, and Build Cost

Designing a SBC that is suitable for the Eastern Mediterranean climatic that can deliver a cooked meal for two people during the Greek outdoor fire ban period (1st May to 31st September) requires several key features including:

- Having a titled (inclined) window;
- Having the ability to be easily directed towards the Sun;;
- Use of local building resources, and where possible use natural sustainable

materials. The design incorporates durable woods rather than cardboard, use recycled flat glass window panes rather than repurposing anti-reflection glass that are hard to find. The use of plastic sheeting is avoided as it degrades quickly in the Mediterranean Sun;

- Portable (size of a suitcase and weight for one person to carry ~10 kg);
- Have a build target cost that is at, or below, present day SBC published build costs.

The SBC is drawn-up using sketched technical drawings for a local carpentry workshop to build an accurate and durable SBC using engineered wood (marine plywood)as given in **Figure 1(a)** and **Figure 1(b)**. The dimensions of the SBC are: width = 32 cm, depth 36 cm, rear height = 29 cm and front height = 20 cm. The walls are constructed from two layers of 9 mm thick marine plywood with an aluminum foil sheet sandwiched between them to act as a heat reflecting barrier. Six mm thick marine plywood is used for the external reflector panel which is hinged at the rear of the SBC with width = 33 and height = 43 cm; area = 0.15 m^2). Aluminum foil sheet is applied to all internal box surfaces and to the external reflector panel. An external reflector brace (14) prevents the panel extending beyond a zenith angle of −10 degrees, not shown **Figure 1(a)**, but is shown in **Figure 1(b)** as component number 14 and in **Table 1**.

The heat absorber plate is made of 0.08 cm thick dark enameled steel sheet cooking vessel with rolled edge (length = 28.5, width = 23, and deep = 6 cm. The vessel has a surface area of approximately 0.154 m^2 and empty mass = 310 g that yields a surface-area-to-mass ratio of sa/ma of approximately 0.513 $m^2 \cdot kg^{-1}$. To reduce heat conduction to the inner box surfaces, a repurposed toaster stainless-steel wireframe suspends the absorber plate from the inner bottom surface by 2 cm which allows warm air convection within.

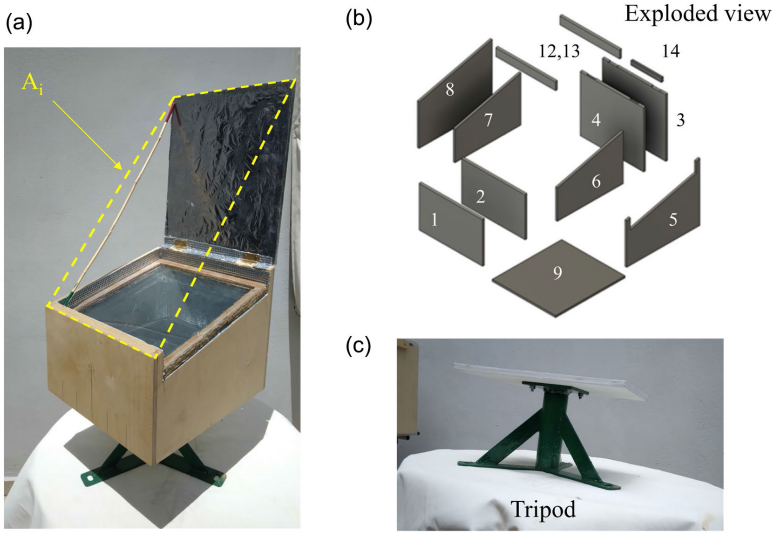

Figure 1. (a)-(c). Photograph of complete SBC with solar incident collection area denoted with yellow dashed lines (a). AutoCAD® exploded view of SBC with numerated component parts (b), and close-up photograph of metal tripod (c).

Table 1. SBC component list.

Item	Number	Material	Description
1	1	Marine plywood	Front out panel
2	1	Marine plywood	Front inner panel
3	1	Marine plywood	Back outer panel
4	1	Marine plywood	Back inner panel
5	1	Marine plywood	Right side outer panel
6	1	Marine plywood	Right side inner panel
7	1	Marine plywood	Left side inner panel with inner reduced height for glass window
8	1	Marine plywood	Left side outer panel
9	1	Marine plywood	Bottom panel
10	1	Marine plywood	External reflector panel
11	1	Marine plywood	Front rail
12	1	Marine plywood	Back rail
13	2	Brass	Folding hinge
14	1	Marine plywood	External reflector brace

The steady-state thermal transmittance (U-value) of a single 4 mm thick window pane is of the order of 5.8 W per m^2 K. Reducing this value is normally achieved by using doubled-glazed units with an air space separation, for example two 4 mm thick glass panes with a 20 mm air separation have a U-value of 2.7 W per m^2 K. For SBC the use of a double-glazed unit over single plane is its does not compromising the glazing handling ability [21] [45] [47] [55]. The double-glazed used here has (width = 31.5, length = 32.5 cm, air separation = 20 mm, and aperture area = 0.1 m^2) is loaded from the right-hand-side of the box with tilt angle of 31 degrees. This requires a 31 degree slot with a depth of 5 cm at the SBC top right-hand-side coupled with two angled rails to provide a structural seat and thermal seal for the double-glazed unit. This novel design allows for the double-glazed unit (or, triple-glazed unit) to be used without affecting the thermal seal between the glazed unit and box the inset design also acts as a windbreak. The 20 mm air space separation between the outer and inner glass is formed from multiple 0.2 cm thick cork strips [24] that are glued together using marine wood glue. To minimize condensation within the doubled-glazed unit, both components are bake in the sunlight for 8 hours to remove water moisture from within the glue. The finally 2 kg glass assembly is made with an edge bias of 31 degrees to match the window frame. **Figure 1(a)** details the upper section of the doubled-glazed unit within the SBC.

The metal tripod is repurposed from a disused TV satellite dish tripod,

alternatively an old car jack will could also suffice. It is modified at a local farm machine workshop with the following dimensions: inner tube (4 cm outer diameter × 8 cm in length) with a flat metal plate (4 × 6 × 0.3 cm), which is welded perpendicular to the free end to which a wooden platform (30 × 25 × 1 cm) that is attached. The competed assembly is then inserted into the tripod where it is free to rotate 360 degrees with a total weight of 2.5 kg **Figure 1(c)**. The initial capital cost and yearly maintenance can be a barrier to the up-take of solar cooking technology. In particular the ability to utilize these hours for people who need to work through these hours, and also cultural food preference. For relatively affluent remote off-grid communities or people simply looking for a sustainable life style the choice of solar cooking can be based upon their environmental believe system rather than an immediate economic necessity.

Table 2 provides the SBC basic build cost and it component cost, based on the 1st June 2024 prices at local carpentry workshops, farm metal workshops, and supermarkets. Using this approach the total cost of the SBC is 107 Euros and when adjusted for US-Dollars (exchange rate 1.09) and for the India-Rupee (exchange rate 89) the SBC cost equates to 116.6 US-dollars or 9523 Rupee.

Table 2. SBC build cost and components based on the 1st June 2024 local prices and their ability to be recycled. * denotes where repurposing of flat glass plan and metal generally requires specialist tools and skills.

Item	Euros	Recyclable
SBC basic build cost	50	-
Aluminum foil (30 m × 30 cm)	4	No
Repurposed 4 mm thick glass planes	0	Yes
Cutting and edge polishing of repurposed glass*	13	-
PVA glue for aluminum foil	5	No
Marine wood glue for double-glazed unit	5	No
Six A4 × 2 mm thick cork sheets	5	Yes
Locally sourced bamboo sticks	0	Yes
Metal cooking vessel	10	Yes
Repurposed metal tripod (without paint)*	15	Yes
Total cost	*107*	-

A direct comparison with other SBC capital cost can be made. For example in India; Poonia, Singh, Santra and Jain (2019) [37] gives a guide price of €45, Kumar *et al.* (2022) [51] provides a cost of €45 to €143; Koshti, Dev, Bharti and Narayan (2023) [31] gives a fabrication cost between €50 to €75 Rupee; and *Kumar et al.* (2023) [52] provides a price guide of approximately 48 US-Dollars. Whereas in Algeria, Benbaha *et al.* (2023) [42] provides a 2023 guide price of €223 to €335. From these reported SBC fabrication costs, the basic fabrication and component cost of the SBC described here is in line with recent reported build costs both India

and Algeria. SBC construction costs, as estimated by Ademe and Hameer (2018) [10], Bhaumik, Sur and Pasi (2018) [20], and Mendoza *et al.* (2019) [5] are not considered as cost have risen significantly after the COVID-19 pandemic.

3. SBC External Reflector Calibration

Solar box thermal performance tests and cooking are performed in Cretan village location which has uninterrupted views of Mt Psiloritis in the east, whilst to the south and west the view is partly blocked by trees of the Mountains that reduce the available cooking period to mornings and afternoon. The following measurements and time of observations are reported in coordinated universal time plus two hours (UTC + 2 hr), and SunCalc software (https://www.suncalc.org) is used to compute the $\delta_{\odot}$ and solar irradiance. Ambient temperature is measured in the shade using a digital thermometer (temperature range −50˚C to 300˚C, with accuracy of 1˚C at 20˚C). For hygiene purposes stainless-steel analogue dial temperature probes are used within the oven: 0˚C to 120˚C, with accuracy of 1˚C, probe for measuring the absorber plate, and a 0˚C to 100˚C, with accuracy of 1˚C, probe for heating water and food.

Locally sourced bamboo sticks harvested from limb of the bamboo plant with typically diameters of 0.4 to 0.5 cm cut into 60 to 44 cm in length and marked accordingly to adjust ϕ_z. This natural and renewable material may be strait or bowed depending on where they are cut from the parent limb. Each stick is set with one end at the lower edge of double-glazed unit and the other end slotted into a recessed hole at the top left edge of the external reflector panel. In this configuration, an increase in bamboo stick length decreases ϕ_z, and increases the solar incident collection area (A_i). Where A_i is the virtual area (diagonal distance between the external reflector panel top edge and the front edge of the SBC multiplied by the SBC width) through which the sunlight passes and allow the SBC to function. **Figure 1(a)** denotes this virtual area with yellows dashed lines.

Figure 2 shows the SBC Sun's geographic azimuth position alignment for ϕ and A_i for the dates of 25.5.2024 and 29.5.2024 at the village location. The alignment is made in two steps. First the shadow alignment method is used at half hour intervals to align the SBC towards the Sun: when there is no shadow on either sidewall of the SBC, the correct azimuth position for a given Sun hour angle is obtained. Second the ϕ_z is adjusted to produce maximum light reflection into the cooking vessel within the SBC. Here it is seen that ϕ_z moves from 28 to −6 degrees in the morning at local noon and back through to 14 degrees. No further measurements are taken after this time as the local foot hills of the White Mountains begin to block the Sun rays. Given this cut-off time the observations produces two symmetrical V shaped curves with their apex of the curve positioned at local noon with a variation of 2 degrees. On the right vertical axis is the estimated value of A_i, as estimated by measuring the diagonal length between the external reflector panel top to the top front edge of the SBC (a steel tape measure provides a linear resolution of 0.5 cm) multiplied by the width of the SBC (0.32 m).

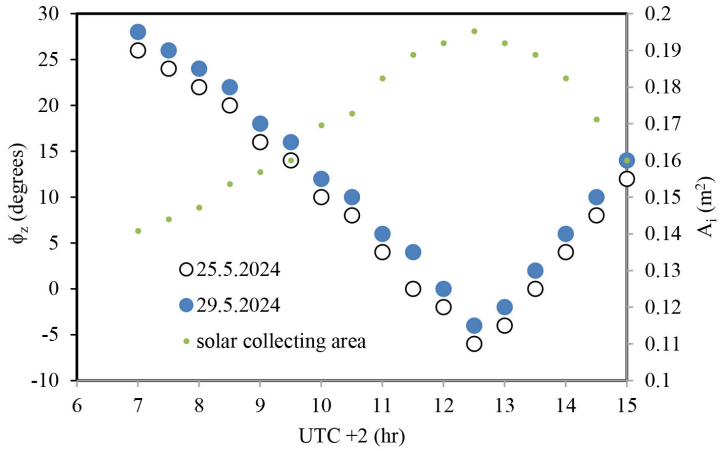

Figure 2. External reflector calibration for the dates for 25.5.2024 and 29.5.2024 at the village location. Primary vertical (left) is ϕ_z, and the secondary vertical axis (right) provides an estimation of A_i.

4. Computation of Instantaneous Power at A_i

In this section two different computer software platforms (SunCalc, and Autodesk Revit® plus insight plug-in) are to estimate the solar power incident upon the SBC.

4.1. SunCalc Open-Source Software

SunCalc software is normally used to find the position of the Sun, an objects shadow length and the solar irradiance at a horizontal surface (measured in $W \cdot m^{-2}$) at a given time of day. In this work this information is the used to estimate the instantaneous power at the SBC virtual A_i surface. For example, for the SBC location on the 27.5.2024 which corresponds to the middle of the dates analyzed in **Figure 3**, the solar irradiance approximates to 940 $W \cdot m^2$ at 9 a.m. and 1026 $W \cdot m^{-2}$ at 12 a.m. Multiplying these values by their A_i values (0.18 and 0.192 m^2) yields 146 and 196 W, respectively.

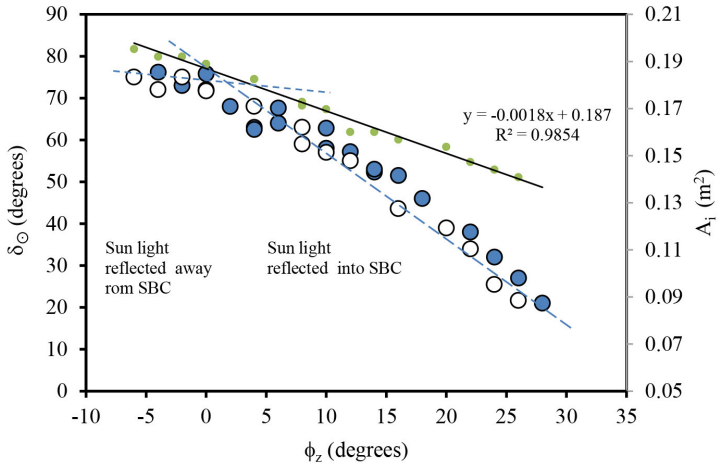

Figure 3. $\delta_\odot$ plotted ϕ_z. Solid trend line represents $\phi_z \sim 0$ to 28 degrees. Open circles 25.5.2024. Blue filed circles 29.5.2024. Dashed trend line represents $\phi_z \sim -6$ to 0 degrees. The secondary vertical axis (right) provides an estimation of A_i.

4.2. Autodesk Revit® Software

Currently the building information modeling (BIM) Autodesk Revit® software license is free to universities and used in many large-scale civil engineering projects [59]. It is thought however, to be rarely used in the solar radiation analysis (SRA) of an object with internal chamber/room dimensions of the order of 33 cm and wall thickness of 1.8 cm. In this work, the BIM software is used to construction a mesh model of the SBC outer physical structure with the external reflector angle adjusted to provide the optimum reflected angle to focus Sun's rays at the center of the internal base surface. The insight plug-in is used to perform SRA of the SBC roof element. In terms of calculation the Insight plug-in uses the Perez model to calculate the incident radiation on an inclined surface [60], and where the computed energy solar insolation values ($J{\cdot}s^{-1} \times s$) are translated from the local solar irradiance values ($J{\cdot}s^{-1}{\cdot}m^2$). Note, that these values do not provide information on how the radiation is attenuated as it passes though A_i nor its distribution within the SBC itself, but does provide an estimation of the solar power incident on the SBC.

Figure 4(a), **Figure 4(b)** shows two Autodesk Revit® 3D views simulation of the SBC-solar coupled system at the site location on the 27.5.2024 which corresponds to the middle of the dates analysed in **Figure 3**. The first simulation is for 9 a.m. with a typical solar irradiance ~ 941 $W{\cdot}m^2$ and second simulation is for 12.0 p.m. with a typical solar irradiance ~ 1026 $W{\cdot}m^2$. Using A_i values of 0.15 m^2 ($\delta_\odot$ =17 degrees) and 0.2 m^2 ($\delta_\odot = -5$ degrees) respectively, instantaneous power values of 118 and 165 W are obtained. The ratio of these values (0.715) corresponds well to their A_i area ratio (0.75).

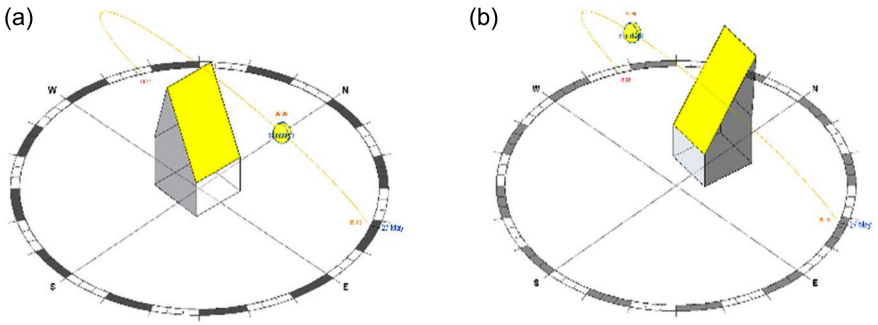

Figure 4. (a) (b). Autodesk Revit® 3D view simulation of SBC-Sun coupled system on the 27.5.2024 at 9.0 a.m. (a), and 12.0 a.m. (b). Their A_i and$\delta_\odot$ values are: 0.15 m^2 and 17 degrees for 9 a.m., and 0.2 m^2 and −5 degrees for 12.00 a.m. The selected area (A_i) for SRA is annotated in the default color yellow.

These input power values along with SunCalc computations are used in section 8 to estimated foodstuff cooking power efficiency.

5. Sensible Temperature Analysis of SBC

The following thermodynamic equations are applied to the sensible temperature measurements to reveal the SBC ability to cook foodstuff when the Sun is shining

and retain heat in off-sunshine periods.

Equation (2) provides a mathematical expression of the first figure of merit, F_1. In this equation the absorber plate temperature (T_{abs}; must be above the boiling temperature of water and measured in ˚C), and T_{amb} is the outside ambient temperature. The difference in these two temperatures is then divided by solar irradiance (H_s; measured in the horizontal plane and expressed in units in W·m^2).

$$F_1 = \frac{T_{abs} - T_{amb}}{H_s}, \text{ measured in units of } ^\circ\text{Cm}^2\cdot\text{W}^{-1} \tag{2}$$

The first figure of merit operates at a high level that captures the balance of heat input to heat loss at the absorber plate at a given point in time. The advantage of using this figure of merit is its ease of use and measurement. However the three terms in the equation is only a snapshot of the heating process and does not capture the difference and nuances between SBC designs: window area, external reflectors that augments the solar heating process. A more realistic first figure of merit includes the solar concentration ratio (A_i divided by A_{abs}), where A_{abs} is the absorber plate area as defined by F_1' [23] and Equation (3) [42]. It is important to note here that the absorber plate may be part of the SBC floor and painted black [23], in this work the absorber plate is a mild-steel plate suspended above the SBC floor that enables the upper surface area to some extend the lower surface area collects solar energy as Sunlight is reflected multiple times from the aluminum lined inner box surface areas. Given that A_{abs} is directly measured and A_i is found using both engineering drawings and measured in practices both F_1 and F_1' are reported here Table 3.

Table 3. SBC F_1 and F_1' results compiled from **Figure 5** and SunCalc software.

Date	Ambient temperature (˚C)	Absorber Temperature (˚C)	Irradiance (W·m^2)	F_1 (˚Cm^2·W^{-1})	A_i (m^2)	A_{abs} (m^2)	F_1' (˚Cm^2·W^{-1})
6.7.2024	28.2	114	1012	0.085	0.19	0.152	0.109
7.7.2024	29	113	1012	0.083	0.19	0.152	0.107
9.7.2024	29.2	115	1012	0.085	0.19	0.152	0.109
Mean	28.8	114	1012	0.084	0.19	0.152	0.108

$$F_1' = \frac{A_i}{A_{abs}} \frac{T_{abs} - T_{amb}}{H_s}, \text{ measured in units of } ^\circ\text{Cm}^2\cdot\text{W}^{-1} \tag{3}$$

The process energy budget required to heat materials (as within many other systems [61] [62]) and cooked foodstuff, can be estimated using the calorimetric open water-dish load method, as mathematically expressed in Equation (4), see for example [10] [12]-[15].

$$P = mC\frac{\Delta T}{\delta t} \tag{4}$$

where P is the applied power (W, or J·s^{-1}), m is the mass (g) of material, C is the

material heat capacity (4.12 $J \cdot g^{-1} \cdot K^{-1}$ for mild steel [63], 4.184 $J \cdot g^{-1} \cdot K^{-1}$ for water, 3.23 $J \cdot g^{-1} \cdot K^{-1}$ for liquid whole egg [64], 4 $J \cdot g^{-1} \cdot K^{-1}$ for pasteurised milk above 30˚C [65]), ΔT is the change in heated material (final temperature minus the initial temperature), and δt is the heating time interval (s). Where T varies with t in a dynamitic reaction, it is normal to take the tangent of the initial temperature curve (t = 0) to obtain *P*. Using this method, P is measured in $J \cdot s^{-1}$ multiplied by process time measured in seconds yields the process energy budget measured in Joules (J), and dividing this value by the mass of material being heated, or cooked, the process energy density, measured in $J \cdot g^{-1}$ is obtained. It is important note that this sequence of calculations are based on sensible heat test measurements, therefore does not provide information on the latent heat of the irreversible chemical and physical process that occurs when cooking foodstuff. The latent heat can only be inferred; however, the calculations do provide information on the energy loss from the SBC to the foodstuff [9] [13] [15] [17] [21] [23] [30] [34] [35] [37] [39] [40] [45]-[47] [50]-[52].

Even though solar cooking uses free and abundant solar energy the cooking process can still produce waste which may or may not be environment begin. In this work the mass-based E-F metrics, or indicator (Sheldon (2018) [58]), and Law (2024) [66] is used in its simplest form Equation (5).

$$\text{E-F} = \text{waste/product, measured in grams} \tag{5}$$

where E-F is the environment Factor, the numerator waste term contains the mass of food waste (eggs shells and egg cartons, and waste cooking water); and the denominator product contains the mass of the edible cooked food. Using this definition the sum of waste mass and product mass equals the total mass of material used in the cooing process. Pre-washing of uncooked food prior to cooking is not included, as it would extend the calculation to a multiple steps calculations [58] [67]. For this study waste/product defines the efficiency of the food cooking process and is used to minimize wastewater in water-stressed communities (where the demand for safe portable water exceeds water supply).

6. SBC Double-Glazed Unloaded Temperature Tests

The unloaded SBC temperature tests were performed in Crete on the following days 6.7.2023, 8.7.2024, and 9.7.204, all of which have high levels of solar irradiance (1012 $W \cdot m^2$). The first test used a fixed $\phi_z \sim 0$ (bamboo length = 57.5 cm) between the hours of 10 a.m. and 3.0 p.m. The second test uses incremental values of $\phi_z \sim 28$, 15, 7, and 0 degrees using bamboo lengths of 44, 51, 56, and 57.5 cm for duration of 1.5 hours each between the hours of 6 a.m. and 3 p.m. The third temperature retention test was performed in the following off-sunshine period of 3 to 6 p.m. with the external reflection panel in the close position with air insulation between the panel and double-glazed unit; the second, with the reflection panel in the close position and 2 cm cloth padding between the double-glazed unit; and third with the external reflection panel in the closed position with 2 cm cloth padding placed and aluminum backed corrugated cardboard on the double-

glazed unit. The temperature profiles of these three unloaded tests are shown in Figure 5 and Figure 6.

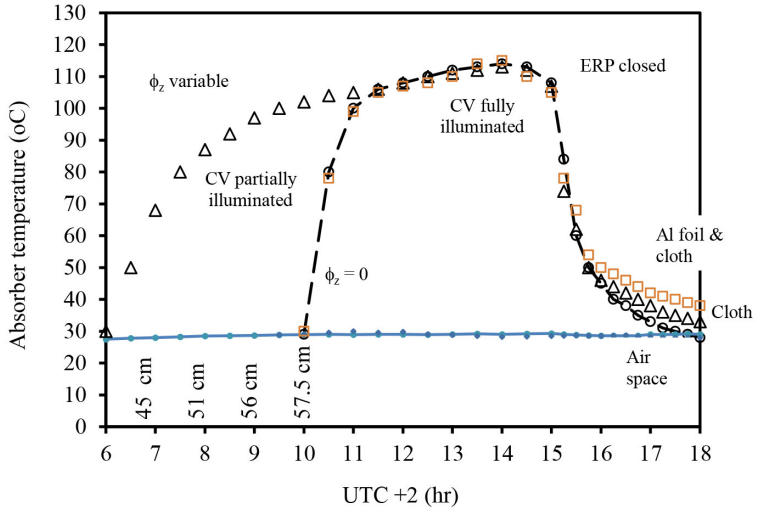

Figure 5. SBC stagnation (unloaded) temperature profiles for: fixed $\phi_z \sim 0$ (black and blue open circles), and variable ϕ_z (green open triangles). Black, blue, and green lines represent their respective shade ambient temperatures. For variable ϕ_z, the Bamboo lengths are also given. The measurements were performed in the village location on the 6.7.2024, 8.7.2024, and 9.7.2024.

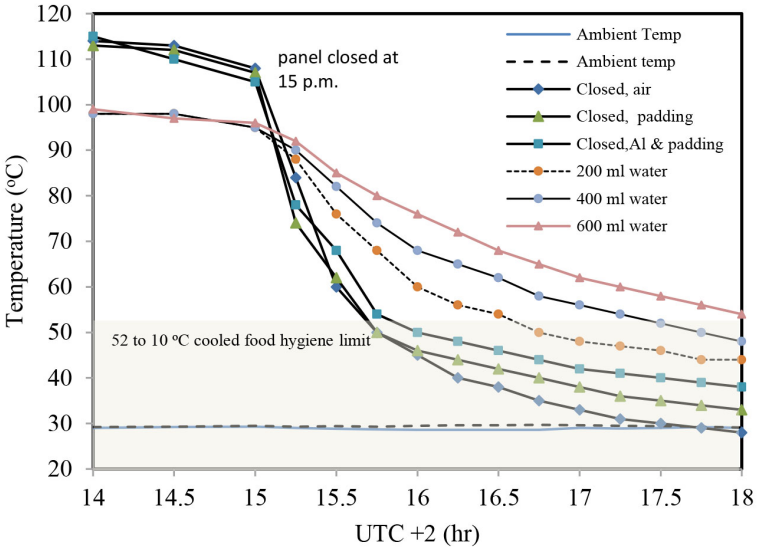

Figure 6. SBC unloaded and loaded (water) cooling temperature profiles after external reflector panel closed at 15 p.m. The closed conditions being: panel closed with air-space, panel closed with cloth padding, and panel closed with cloth padding plus aluminum backed corrugated cardboard. The grey area denotes the temperature region where cooked food should not be kept stored, but rather refrigerated [4].

In Figure 5 the first feature of note is that all test ambient temperatures profiles are relatively flat within a variation of 28˚C to 30˚C. The variable external reflector

panel ϕ_z test begins at t = 6 a.m. with an absorber plate initial temperature slope ($\Delta T/\delta t$) of some 0.0105˚C·s^{-1}. Between t = 8 and 11 a.m. the rate is approximately 0.33˚C·min^{-1} at which point a small but observable inflection in the heating profile that reaches a maximum steady-state equilibrium temperature of 114˚C to 115˚C (Table 3) from where the hills and trees at the test location begin to shadow the sunlight a result the absorber plate temperature falls. At t = 3 p.m., the external reflector panel is closed creating an air space between the panel and the double-glazed unit which induces an initial rapid fall in absorber plate temperature of -0.025˚C·s^{-1} then cools at slower rate until equilibrates at 28˚C at t = 18 p.m., where the measurement is stopped.

The fixed ϕ_z = 0 degrees (bamboo length = 57.5 cm) the temperature profiles begins at t = 10 a.m. with an initial temperature slope ($\Delta T/\delta t$) of some 0.019˚C·s^{-1}, or nearly double the initial rate of the variable ϕ_z. At t = 11 a.m. through to t = 14 p.m. the temperature profiles follows the variable ϕ_z measurement reaching a maximum temperature of 114˚C to 115˚C (Table 3) where the local hills and trees begin to shadow the Sun to induce a drop in absorber plate temperature. At t = 15 p.m. the external reflector panel is closed with an air space between the panel and the double-glazed unit induces a rapid fall in absorber plate temperature of −0.02˚C·s^{-1} then cools at a slower rate to equilibrate 28˚C at t = 18 p.m., where the measurement is stopped.

In the hours of t = 3 to 6 p.m. the absorber plate cooling rate is shown with the external reflector panel in the closed condition (air-space, 2 cm cloth padding, and aluminum backed corrugated cardboard with 2 cm cloth padding). Here it is observed that cooling rate is retarded for the sequence: air-space, cm cloth padding and cloth padding plus aluminum back corrugated cardboard. These cooling conditions are further explored with a water load in Figure 6.

The data in Table 3 lists the SBC temperature data, the Sun's irradiance on the day of measurement and computed F_1 and F_1' values with mean values of 0.084˚Cm^2·W^{-1}, and 0.108˚Cm^2·W^{-1}, respectively. Here the increased value of F_1' is only due to the mean solar concentration ratio term. It is noted that the mean F_1 value is lower than most reported SBC values, however it is comparable to a SBC with four external reflectors [17] [47], a SBC with a tilted window set at latitude 35˚C of the test location [50] and rectangular cavity SBC when compared to compared to trapezoidal cavity SBC [68]; the mean F_1' value is within the accepted norm of the first figure of merit standard.

Retained-heat within SBC in off-sunshine hours

When physical structures or clouds obscure sunlight the SBC can be converted to act in a retain-heat mode. For a SBC with at least one external reflector panel this is achieved by simply closing one of the panels onto the window aperture. How well this operation works in maintaining the absorber plate, and cooked food temperature is a key question, the outcome of which determines the usefulness of the SBC in temperate zones.

Figure 6 shows the three unloaded absorber plate cooling temperature profiles along with three loaded (200, 400, and 600 ml, or grams, of water) absorber plate

cooling temperature profiles. In all six measurements the ambient temperature profiles varying between 28˚C and 31˚C. As previously shown in **Figure 5** the unloaded absorbed plate temperatures have an initial cooling rate of −0.024 ± 0.02˚C·s^{1}. These rates are followed by slower cooling rate of −0.15 ± 0.0015˚C·min^{-1} and trend towards ambient temperature as the absorber plate equilibrates with its surrounding temperature. For example the temperature values at t = 18 p.m. are 28˚C for simple closed panel, 33˚C for closed panel with cloth padding, and 38˚C for closed panel with cloth padding plus aluminum foil backed corrugated cardboard.

The loaded absorber plate temperatures profiles begin typically at 98˚C to 99˚C. In each case the external reflector panel is closed with varying degrees of insulation: first air, second cloth padding, and third cloth padding with aluminum foil backed corrugated cardboard. In this sequence the initial temperature duration is short followed by an increasingly linear behavior as the volume or mass of water increases from 200 ml (0.2 kg) to 400 ml (0.4 kg), and 600 ml (0.6 kg). In the latter regions the cooling is some 13 ± 0.4˚C·hr^{-1}. Finally the temperature falls to 44 through 48˚C to 54˚C. These results indicate the high absorber plate sa/ma (0.645 m^{2}·kg^{-1}) dominates the initial cooling period. Whereas the progressively decreasing sa/ma water loads (0.203, 0.114, and 0.085 m^{2}·kg^{-1}) determines the latter period of the temperature cooling profile.

As regarding to cooked food storage and hygiene, a SBC generally protects cooked food from wind contaminate. According to Solar Cooker International [4] a good food hygiene guide may be stated as:

"*As with any cooking method, cooked food that is allowed to cool to temperatures between* 52˚C - 10˚C (125 - 50˚F) *for a period of time may contain bacteria that can spoil food and lead to food poisoning. Food that stays in this temperature range for more than four hours should be discarded*".

From these working practices cooked foodstuff, as simulated by a water load of 600 ml, stored within an unopened SBC more can be stored for two to three hours before serving; otherwise the foodstuff should refrigerated for later serving.

7. Sensible Heat Test Experiments for Eggs without Water, and Foodstuff Using Water

Successful solar cooking generally involves the heating of foodstuff to a temperature that induces a chemical and physical irreversible change in its constituent parts that allows food to be safely eaten. In water-stress communities successful solar cooking need to involve the minimum use of water. Therefore understanding of solar cooking without and with water becomes an important issue. For solar cooking of whole eggs without water it is known that they undergo a liquid-to-solid transition a process called protein denaturation; typically the inner yellow yolk begins to denature at 62˚C and solidifies at around 70˚C and the protective outer translucent albumen denatures in the range of 60˚C to 84˚C [68] [69]. However, cooking of rice and pasta involves the use of water where individual rice grains, or length of dried-pasta, undergo a glass to rubbery transformation and

swelling when subjected to heated water, and hopefully a flavorsome taste [70].

This section details a series of solar cooking experiments of whole eggs-without water, and white medium-grain rice, dried pastitsio #2 pasta, and Brown lentils with water. The following solar experiments are informed by published solar cooking data compiled from SCI data [4] and eleven scientific journals [11] [13] [16] [21] [22] [24] [26] [33] [38] [44] (**Table 4**). N.B. the work of Saxena, Goel and Karakilcik "Solar food processing and cooking methodologies" (2018) [5] is not listed, as no solar cooking food recipes were given]. The cooking data listed in **Table 4** if not complete does provide a starting point.

Table 4. Solar cooking data for eggs, rice, pasta, and lentils compiled from SCI and eleven scientific journal published between 2004 and 2023.

Author Solar cooker type	Date	Water + eggs time	Water + rice mass time	Water + pasta mass time	Water + lentils mass time	Ref
Nahar *SHBC*	2003	_	250 g + rice not reported 2.5 hours	_	_	39
Solar cooker international *SBC*	2004	No water >1 egg 1 to 2 hours	$1\frac{1}{2}$ - 2 to 1 ratio 1 to 2 hours	Heat water then add sun warmed pasta 10 to 15 minutes	2 or 3 to 1 ratio 2 to3 hours	4
Adetifa & Aremu *Double exposure SBC*	2016	500 g + 4 eggs 50 minutes	260 g + 200 g jollof rice 120 minutes	_	_	23
Soe, Win and Min *SBC**	2019	Water? 9 eggs 1.5 hours	Not reported white rice 2.25 hours	_	_	11
Zafar, *et al.* *L-shape SBC***	2018	_	Not reported white rice ~60 minutes	_	_	34
Bhaumik, Sur and Pasi *SBC****	2018	No water 2 eggs 1 - 2 hours	Not reported 1.5 - 2.5 hours	_	_	20
Soro *et al.* *SBC*	2020	0.5 l water 2 eggs 2.5 hours	not reported 2 hours 20 minutes			25
Al-Nehari *et al.* *SBC*	2021	_	Not reported ~2 hours	Not reported ~2 hours	_	27
Wassie *et al.* *SBC*	2022	_	I.5 kg + 1 kg white rice 53 minutes	1.5 L water 1 kg pasta 17 minutes	_	14
Manohar *et al.* *Double exposure SBC*	2023	_	Not reported white rice ~45 minutes	_	_	22
Vaidya *et al.* *SBC*	2023	_	350 g + 250 g white rice 130 minutes	_	350 g + 250 g 130 minutes	16
Belatrache *et al.* *SHBC with 3 reflectors & 2 wings*	2024	1.5 kg + 7 to 10 eggs 1 hr 45 minutes	_	_	1.5 k g + 1 kg 135 minutes	45

* Cooked prawns in 4 hours. ** Cooked grilled chicken in 90 minutes. *** Cooked fish and chicken curry.

In the case cooking of whole eggs to produce edible hard-boiled egg [4] [11] [22] [24] [44] water appears optional with the cooking time ranging between 1 to 2 hours 20 minutes.

For solar cooking of rice, ten references [4] [11] [13] [16] [20] [21] [24] [26] [33] [38] out of the eleven do not provide information on the type and variety of rice used, only Adetifa & Aremu (2013) [22] reports that they used long-grain Jollof rice. Where white rice is recorded this is taken from photographs within the reference. Given this limited data the water ratio appears to be related to the water absorption method (typically 1.5 to 2 parts water to 1 part rice) with cooking time ranging from 1 to 2.5 hours without a clear correlation to the type of solar cooker used. It is also noted that Manohar *et al.* (2023) [21] provides in detail the absorber plate temperatures relating to the opening and closing of the cooking vessel lid.

For the three reports on dried-pasta, SCI (2004) [4] recommends heating the water first whilst leaving the dried-pasta to warn in the sun and once the water is boiling add the dried-pasta to rehydrate resulting in a minimal cooking time 10 to 15 minutes. Al-Nehari *et al.* (2023) [27] do not report the amount water or pasta used but does report a cooking time of 2 hours which suggest the dried pasta is place in water then solar water-pasta mixture heated. Wassie *et al.* (2022) [14] gives the water and pasta ratio as 1.5 to 1 with a cooking time of 17 minutes which implies the pasta was added to solar heated water, as in the case of SCI.

Brown lentils are an edible seed originating from legume plants. To cook these seeds requires large amount of water to remove anti-nutrients, and reduce their uncomfortable effects, Martins (2023) [71]. Solar cooker international [4] reports using SBC to cook a Variety of lentils types with red lentils taking the longest to cook but its time can be reduced by pre-socking (**Table 4, row 3; column 6**). Vaidya, Rathod and Channiwala (2023) [16] used a SBC to cook 350 g of water with 250 g of Brown lentils with cooking time of 130 minutes (**Table 4, row 12; column 6**). Belatrache *et al.* (2024) [43] has also used and SHBC with wings to cook 1 kg of brown lentils in 1.5 kg of water with a cooking time of 135 minutes at a solar irradiance of 1050 $W \cdot m^2$ (**Table 4, row 13; column 6**).

From this simple review of solar cooking data it is clear the data is not complete and is carried out in single and double exposure SBC, SHBC, all with their own cooking vessels. To provide a consistent cooking approach that will yield meaningful cooking data performed in one SBC and one single cooking vessel between 28.7.2024 and 19.8.2024 at one site location. Within the cooking times reported here the solar irradiance varied between 910 and 1010 $W \cdot m^2$.

Hard-boiled eggs (without water) for salad recipe

Three room temperature whole eggs (total 162 grams) are placed in a cut down cardboard egg box container, which is placed on the solar preheated absorber plate, temperature of 95˚C. The cardboard egg box is used to stabilize the eggs on the absorber plate and prevent the egg shells from burning **Figure 10(a)**.

Figure 7 shows the solar cooking temperature profile of one whole egg (blue filled diamonds) out of 3 eggs. At the start of the heating process (t = 0 minutes)

the initial temperature increases at 0.024 $\Delta T/\delta t$ for the first 30 minutes of heating, where evoking the work of Fernandez-Burgos *et al.* [72] it is reasonable to assume the heat loss is zero, and by extension, from t = 30 minutes the temperature rate rise slows due to heat loss to the eggs begins. Further on at t = 90 minutes, the egg is judged to be cooked (black filled circle). Importantly the final cooked temperature (90˚C) is some 20˚C above the yolk solidification temperature and 16˚C above the albumen denaturation temperature. Given this analysis the egg temperature profile classified in to two time periods: t = 0 to 30 minutes is the heating period, and t = 30 to 120 minutes is the cooking period. **Figure 10(b)** shows the cooked egg sliced open to reveal the outer white and the inner yellow yolk.

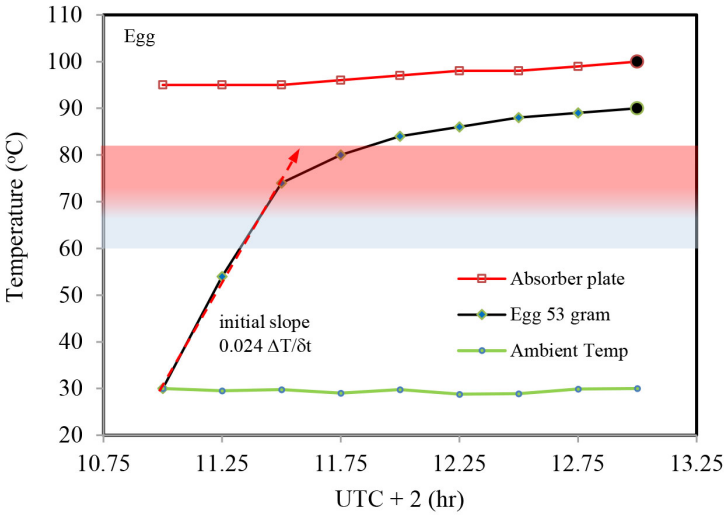

Figure 7. Solar box cooker temperature profile for one out three hard-boiled eggs without water (blue filled diamonds), Open squares represent the absorber plate temperature. Black filled circle denotes the completion of the cooking time. The transparent blue to red band represents yolk and albumen denaturation temperature ranges. Green filled circles represent the ambient temperature on the 27.7.2024.

White medium-grain rice water-absorption recipe

A 600 ml (458 gram) non-black painted Pyrex glass cooking vessel is placed on the absorber and solar preheated to a temperature 95˚C. Add 200 g of water and 100 g of uncooked white medium-grain rice and close the vessel lid. **Figure 8** shows the rice-water mixture (open diamonds) having an initial (t = 0 to 30 minutes) temperature rate rise of 0.025 $\Delta T/\delta t$ from where the rate slows to temperature of 94˚C at t = 90 minutes where the rice is judged to be cooked (black filled circle). Also see **Figure 10(c)**. In this temperature period the absorber plate temperature reacts to the addition of rice (red dashed trend-line) by falling to 80˚C at t = 15 minutes; then steadily increases again. Note also that when the rice is added to the solar preheated water cooking time is decreased to 50 minutes with a final temperature of 96˚C (black filled circle). Similar drops in absorber plate water temperature as the rice is added have been reported by Manohar *et al.* (2023)

[21] and is considered to be caused by the release of hot air as the solar cooker and cooking vessel are opened to allow the addition rice.

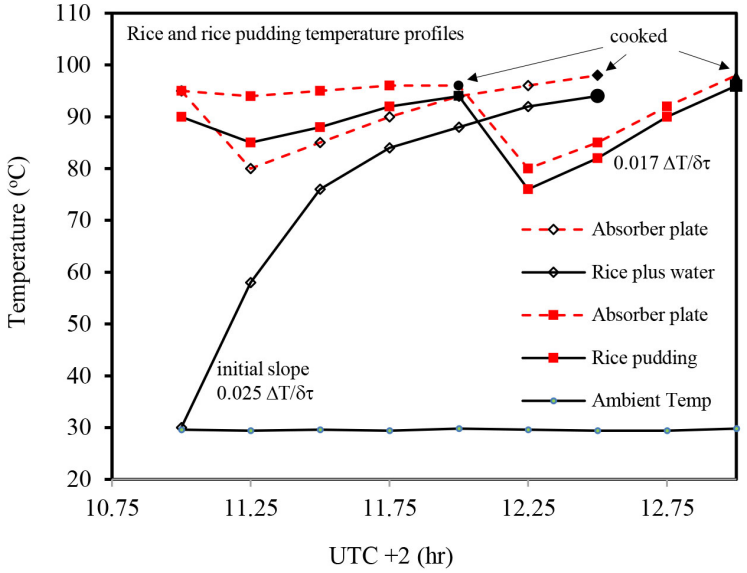

Figure 8. SBC temperature profiles for one-step white medium-grain rice; non preheated water (open diamonds) and preheated water two-step rice pudding (red filled squares). The dashed trend-lines represent their absorber plate temperatures. The black filled circles denoted the final rice cooking time. Green filled circles represent the ambient temperature on the 28.7.2024, and 29.7.2024.

White medium-grain rice pudding water and milk absorption recipe

This is a two-step cooking process with the first step following the rice water absorption recipe **Figure 8**. The second-step involves opening vessel lid and stir-in150 g of milk with a fat content <1.5% by weight, and sugar to taste. During this operation the temperature of both the absorber plate and the rice mixture falls [21]. Upon closing the cooking vessel lid and refitting the double-glazed unit heat is once again trapped within the SBC resulting in absorber plate and rice mixture temperature stabilizing and within 15 minutes begin to increase once again At this point the rice mixture linearly increases for a further 45 minutes to a temperature of 96˚C where it is judged to be cooked (black filled triangles). This gives a cooking time, with one brief opening and closing of the cooking vessel of two hours. When the initial water solar heating time is added, a total cooking time of two hours 30 minutes achieved.

pasta #2 water absorption recipe

A 600 ml (458 gram) non-black painted Pyrex glass cooking vessel containing 100 g of cut dried-pasta (typically 6 cm in length and 4.5 mm in diameter) plus 350 g of water is paced on the solar preheated absorber plate temperature of 95˚C. The temperature profile is show in **Figure 9** as blue triangles. Here the pasta-water mixture temperature initially increases at a rate of 0.024 $\Delta T/\delta t$ from t = 0 to 30 minutes with the usual temporary fall in absorber plate temperature response. After which both temperature profiles gradually increase to t = 60 minutes where

the pasta has passed through the glass to rubbery transformation and is judged to be cooked with a soft *al dente* texture. Weight and volumetric expansion measurements reveal that 165 g of the original 350 g of water has been absorbed by the pasta, and the #2 tubes have swelled from 4.5 to 7 mm in diameter, length has increased by some 50% Figure 10(d).

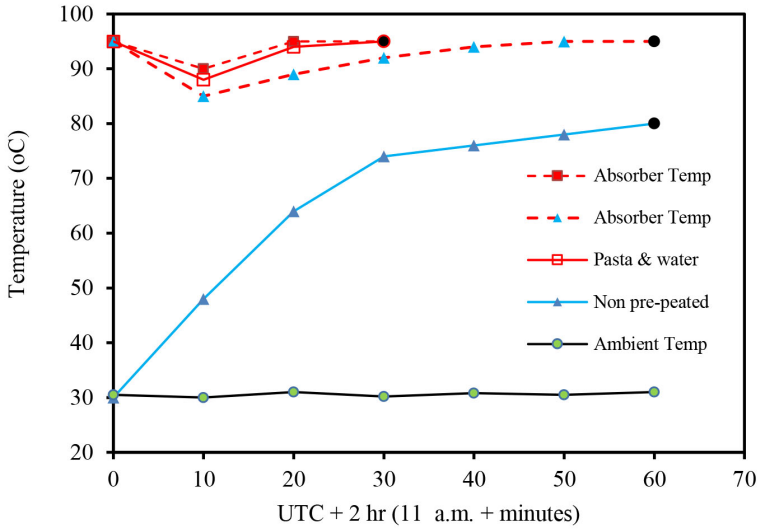

Figure 9. SBC temperature profiles obtained during the cooking of pasta-water mixtures. Preheated water (open squares). None preheated water (blue triangles). Their absorber plate temperature profile (dashed trend-line). The black filled circles denoted the final pasta cooking time. Green filled circles represent the ambient temperature on the 30.7.2024 and 5.8.2024.

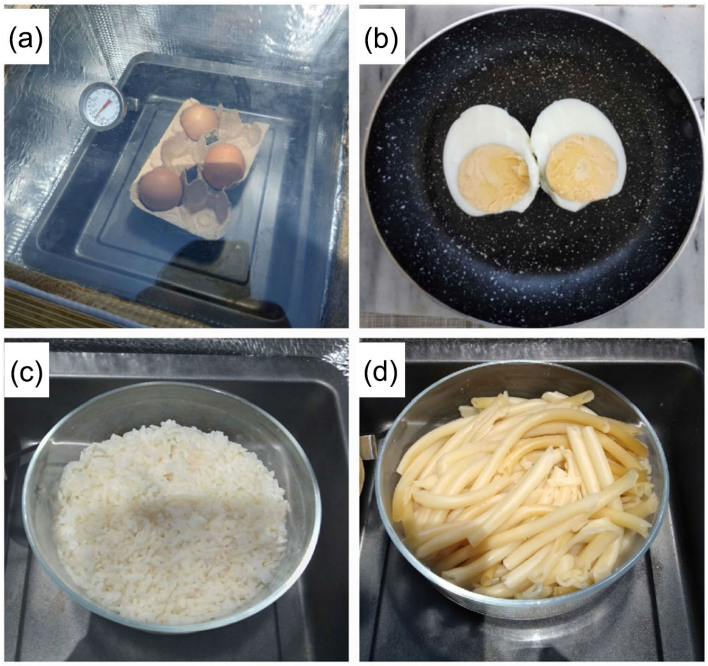

Figure 10. (a)-(d). Photograph of SBC cooking of eggs (a) slice cooked eggs (b), cooked white medium-grain rice (c), cooked #2 pasta (d).

A further study involved the same cooking vessel to which 350 g of water was added and this then solar heated on the absorber plate to a temperature of 95˚C. To this is added 100 g of the dried pasta and close the vessel lid and the solar window. The temperature profile is show in **Figure 9** this time as open squares with red trend-line. Note when the cooking vessel is opened and the pasta is added both absorber palate and water temperature fall due to the release of hot air [21] then gradually increases to t = 30 minutes where it has undergone the glass to rubbery transformation. At this point the pasta is judged to have a soft Al Dente scale (soft to hard transition in the radial direction [70]).

Three brown lentil cooking recipes were evaluated using the SBC, as follows:

Brown lentils recipe 1. Soak 100 g of brown small (typically 4 × 5 × 2.5 mm) lentils for 2 hours in 300 g of water within a 600 ml (458 gram) non-black painted Pyrex glass cooking vessel. At the same time solar preheated the absorber plate to a temperature 95˚C. Once the soaking period is complete, place the cooking vessel in the SBC and close the window. The results are given **Figure 11** and the data is listed in **Table 5**. The sensible temperature data shows the lentils mixture (open diamonds) has an initial (t = 0 to 30 minutes) temperature rate rise of 0.02 $\Delta T/\delta t$ from where the rate slows to temperature of 94˚C at t = 105 minutes. At this point the lentils have swollen double in volume and are judged by pressing a few lentils between finger and thumb to check they are cooked (Vaidya, Rathod and Channiwala (2023) [16] (black filled circle). The photograph insert shows the relative size of uncooked lentils and the cooked lentils.

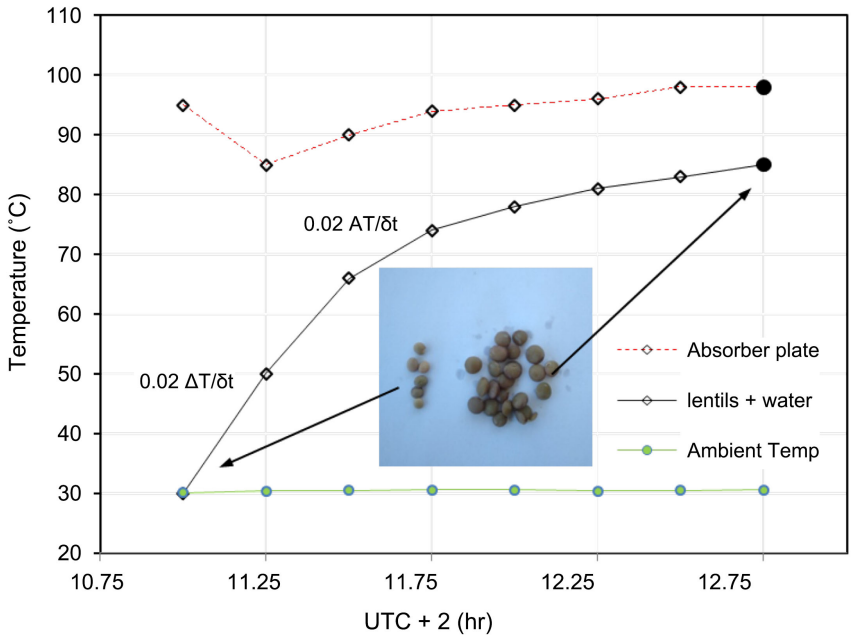

Figure 11. SBC temperature profiles obtained during the cooking of pre-soaked lentils (open diamonds). The absorber plate temperature profile (dashed trend-line). The black filled circles denoted the final lentils cooking time. Green filled circles represent the ambient temperature on the 7.8.2024.

Table 5. Estimated cooking power, cooking energy budget and cooking energy density for: eggs, white medium-grain rice, rice pudding, and pastitsio # 2 pasta.

Food	Food (g)	Water (g)	$\Delta T/\delta t$	Cooking time (s)	Cooking power ($J \cdot s^{-1}$)	Cooking Energy (kJ)	Energy density ($kJ \cdot g^{-1}$)
Three whole eggs	162	None	0.024	7200	13.07	94.1	0.580
White medium-grain rice	100	200	0.025	7800	32.07	115.48	0.385
Pastitsio # 2 pasta	100	350	0.0277	5400	52.3	94.14	0.209
Pastitsio # 2 pasta drained	100	165	0.0277	5400	52.3	94.14	0.355
Brown lentils	100	300	0.02	6300	33.47	210.80	0.527
Brown lentils	100	200	0.019	6300	24.40	153.762	0.512

Brown lentils recipe 2. Soak 100 g of brown small (typically 4 × 5 × 2.5 mm) lentils for 2 hours in 200 g of water within a 600 ml (458 gram) non-black painted Pyrex glass cooking vessel. At the same time solar preheated the absorber plate to a temperature 95˚C. Once the soaking period is complete, place the cooking vessel in the SBC and close the window. The data is listed in Table 5 and shows the lentils mixture (open diamonds) has an initial (t = 0 to 30 minutes) temperature rate rise of 0.019 $\Delta T/\delta t$ from where the rate slows to temperature of 86˚C at t = 105 minutes. At this point the lentils are swollen double in volume and are judged by pressing a few lentils between finger and thumb to check they are cooked [16].

Brown lentils recipe 3. Soak 100 g of brown small (typically 4 × 5 × 2.5 mm) lentils for 2 hours in 150 g of water within a 600 ml (458 gram) non-black painted Pyrex glass cooking vessel. At the same time solar preheated the absorber plate to a temperature 95˚C. Once the soaking period is complete, place the cooking vessel in the SBC and close the window. The data is not reported, but does have initial lentils (t = 0 to 30 minutes) temperature rate rise of 0.019 $\Delta T/\delta t$ from where the temperature rises to of 85˚C at t = 120 minutes. Visually, at this point some of the lentils are swollen double in volume and some are not and the dish is judged to be incompletely cooked through due to the lost of water between the lentils. Here it is reasonable to assume the lost of water is due absorption and evaporation.

8. Food Cooking Power, Energy Budget, and Energy Density

This section uses the sensible heat test results obtained in section 7 to estimate the food cooking power required for whole eggs-without water and the following with water: white medium-grain rice, rice pudding, pastitsio #2 pasta and Brown Lentils. The cooking energy budget and cooking energy densities are also estimated. The calculations are based on Equation (4) where it is assumed that the power is distributed evenly throughout the cooked food. Table 5 lists the food type mass, water mass and $\Delta T/\delta t$, and cooking time used to estimate the cooking power (row 6), cooking energy (row 7), and cooking energy density (row 8).

An estimation of the additional cooking power and cooking energy budget for

processing of the cooked white rice into rice pudding is listed in Table 6. Here the knowledge that milk is made of water and total solids (fats, proteins, lactose, and minerals) and has stable heat capacity of 4 $J \cdot g^{-1} \cdot K^{-1}$ between 30˚C and 60˚C to 90˚C when the fat content <3.5% weight (Munir *et al.* (2016) [65]) is used.

Table 6. Estimated cooking power and cooking energy budget for transforming cooked white medium grain rice into rice pudding.

Food	Milk (g)	Additional cooking time (s)	Additional cooking power ($J \cdot s^{-1}$)	Total cooking power ($J \cdot s^{-1}$)	Total cooking energy (kJ)	Total energy density ($kJ \cdot g^{-1}$)
Rice pudding	150	3600	5.111	37.188	133.874	0.243

The cooked food data presented in Table 5 and Table 6 are placed into context using process (cooking) energy phase-space projection; Law (2024) [66], and Law and Dowling (2023) [73] as shown in Figure 12. In this projection the cooking energy budget (kJ) plotted on the horizontal axes and the cooking energy density ($kJ \cdot g^{-1}$) is plotted the vertical axes. Here the cooked eggs without water (black filled circle) and rice, rice pudding and pastitsio #2 pasta all may be considered to utilize the absorption method of cooking, for this reason a linear regression trend-lined ($y = -0.0028x + 1376$, solid trend-line) is fitted to this group with a linear regression coefficient $R^2 = 0.9976$. The non-absorption method used to the pastitsio #2 pasta (red filled square) and Brown lentils (red filled diamonds) data points are visually located furthest away from the trend-line, but as the excess cooking water is reduced their data points approach the absorption method trend-line at a point between the egg and rice coordinates. Finally for these groupings the solar cooking process operates in the 90 to 150 kJ range with a cooking process energy density 0.2 to 0.6 $kJ \cdot g^{-1}$.

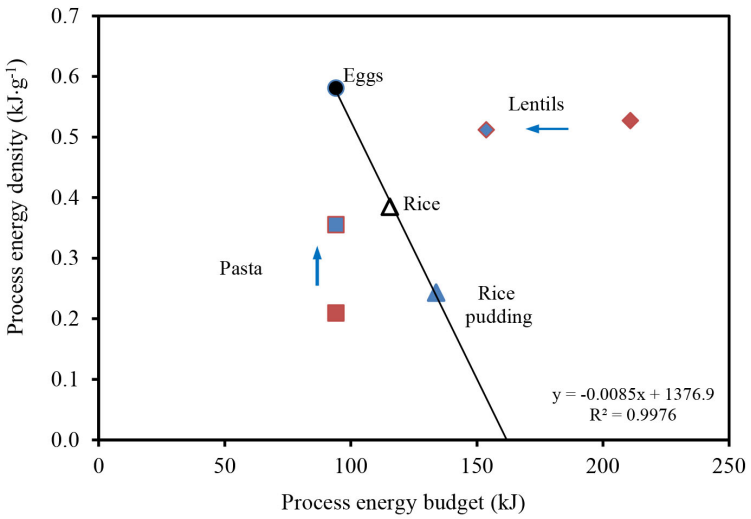

Figure 12. Process (cooking) energy phase-space projection of: cooked eggs without water, white medium-grain rice, rice pudding and pastitsio #2 pasta cooked using the absorption method and: pastitsio #2 pasta and brown lentils cooked in excess water.

9. Food Cooking Power Efficiency

An estimation of the food cooking power efficiency (FCPE) is an important parameter for comparing different SBCs and the future design improvement. One way of obtaining an estimation of the FCPE is to explore the solar input power at the start of the cooking process divided by the initial calorimetric value obtained from the initial temperature slope ($\Delta T/\delta t$), expressed as percentage for the range of foodstuff studied here. In this work the solar input power is estimated by dividing the date and time stamped solar irradiance at by the time stamped A_i (0.192 m^2).

Table 7 shows the result of these calculations for SunCalc and Insight plug-in software at 11 a.m. for three whole eggs (Figure 7), White medium-grain rice (Figure 8), pastistio #2 pasta (Figure 9), and Brown Lentils (Figure 11). The first feature of note this that the three cooked eggs exhibits a low FCPE (6.53%), here it is reasonable to assume that their combined mass without water (162 g) and is much lower than the rice, pastistio and lentils. Given the three eggs use a low proportion of the cooking vessel volume, this suggests that more eggs could be cooked as demonstrated by [11] [44]. The second feature of note is that the SunCalc software provides an approximate 1/3 lower valves as compared the Autodesk Revit® Insight software calculated values. It is thought that the mains reason being that the SunCalc irradiance values are derived from calculations performed on the earth's horizontal plan then multiplied by the SBC A_i. Whereas the insight plug-in start with the Sun irradiance on the earth's surface, then uses the Perez model to calculate the incident radiation on the mimicked A_i inclined surface [60]. For this reason Table 7, column 5 gives the FCPE as an estimated range that combines the two software calculations.

Table 7. Food cooking efficiency using SunCalc and Insight plug-in solar input power for cooking or three whole eggs on 7.8.2024, White medium-grain rice on the 28.7.2024, pastistio #2 pasta on the 30.7.2024 and Brown Lentils on 7.8.2024.

Food	Date 11 a.m. start time	SunCalc Solar irradiance * A_i @ 11a.m.	Insight plug-in Solar irradiance * A_i @ 11a.m.	FCPE (%)
Three whole eggs	27.7.2024	199	147	6.5% to 8.9%
White medium-grain rice	28.7.2024	199	147	16% to 21.8%
Pastitsio # 2 pasta*	30.7.2024	199	147	26.2% to 35.5%
Brown lentils**	7.8.2024	193	143	17.3% to 23.4%

*Data from Table 5, row 4 (pasta: water = 100:350), ** Data from Table 5, row 6 (lentils: water = 100:300).

10. Mass-Based Waste/Product Metrics

Table 8 shows the basic input mass data that is required to calculate the mass-based waste/ product efficiency for each of the recipes For example, solar cooking of three eggs-without water in 7200 s (120 minutes), a simple waste/product value

of 0.122 is obtain. Here the egg shells and cardboard egg carton is considered to be beneficial to the environment and arguably most people would considered this waste as vegetable patch or garden composite. Therefore a recycled waste/product value would equate to zero. Compared to cooking whole eggs in water, Belatrache *et al.* [44] cooking of 10 whole eggs in 105 minutes equates to a simple waste (1.5 kg + 0.05 kg egg shell)/product (0.53 kg hard boiled eggs −0.05 kg egg shells) of 3.29 or 3.125 when the eggs are recycled. The question of how to recycle the 1.5 kg of prolonged boiling (105 minutes of) depends on sanitary standards of the water source [74].

Table 8. Mass-based waste/product metrics.

Target cooked food	Food mass (g)	Eggs & box mass (g)	Water/milk mass (g)	Product mass (g)	Waste mass (g)	Simple waste/ product	Recycled waste/ product
3 hard boiled eggs	160	20	non	180	20	0.122	0
White medium-grain rice	100	_	200	300	0	0	0
Rice pudding	100	-	300	400	0	0	0
Pastitsio #2 pasta	100		350	285	165	0.578	0
Brown lentils	100	-	300	400	185	0.462	0
Brown lentils	100	-	200	300	100	0.333	0

Extending this environment mathematical process to solar cooking of White medium-grain rice and rice pudding absorption method of cooking there is no waste generated and the simple waste/product equates to zero.

Solar Cooking of 100 g of pastitios #2 pasta can produce a hot excess of starch infused water. In the example given here the waste/product value is of the order of 0.578 however resourceful cookery would mean that the water is used in accompanying recipe. For example, in the wilting spinach leaf for a garnish, added to a tomato sauce or soup to yield a recycled waste/product metrics of zero.

It is known that cooking of lentils and other pulses require plenty of water. In the example given the excess cooked water can be 100 to 1885 g per 100 of Brown lentils which equates to simple waste/product value of 0.33 to 0.462. Again a cook may recycle this hot protein and oligosaccharides infused water in vegetable stock or another meal. Martins *et al.* (2023) [71] has also shown that this excess water can be valorized and effectively repurposed as microbiological growth media for lactic acid bacteria.

11. Summary and Future Work

This work describes the food cooking performance of an inclined widow solar box cooker designed for Mediterranean latitudes (35.31˚N, 24.31˚E) within the period of May to August which includes the summer solstice (21st June). This is achieved by showing how the Sun illuminates the inner surface of the SBC. Experimental

measurements have been performed to reveal how the external reflector needs to be adjusted to couple to the Sun's position in the sky throughout the duration of the solar cooking period. Computer-based SRA has been used to estimate the SBC solar input power and found to be in the ordered of 141 to 204 W between 9.0 a.m. to 12.0 p.m. on the 27.5.2024. Using this knowledge, food cooking experimental variables (solar cooker-type, cooking vessel, date, time, and location) are minimized to allow a meaningful comparison to be made between a range of household meals for two people to be made. The foods investigated are: whole eggs-without water, and the following with water; White medium-grain rice, rice pudding, pastitsio #2 pasta and Brown small lentils. The food cooking metrics used are the food cooking power (W), cooking energy (kJ), energy density ($kJ \cdot g^{-1}$), and mass-based waste/product efficiency. For completeness, SBC spot values for first figure of merit (F_1') and corrected solar collecting area (F_1') are also given.

The SBC food cooking results obtained for three whole eggs-without water, and the following with water; White medium-grain rice, rice pudding, pastitsio #2 pasta and Brown small lentils are as follows: Food cooking power of 13 to 53 $J \cdot s^{-1}$, cooking energy of 94 to 210 kJ and energy densities in the range of 0.2 to 0.6 $kJ \cdot g^{-1}$). It is also found that the food cooking power efficiency varies between 6 to 8.9% for three whole eggs-without water, and 16% to 35.5% for rice, pasta, and lentils cooked in water.

To the authors knowledge Autodesk Revit® BIM software and the SRA Insight plug-in, that licensed free to universities, has been used to simulate the SBC-solar coupled system and the SBC solar input power. Where license conditions prohibit its used, such as for individuals and communities that are not affiliated to a university, SunCalc open source software (free of charge and requiring no login or password access) provides a systemic 1/3 lower solar irradiance valve. Given this knowledge, people operating SBCs around the world (for example Mexico, Greece, India and Malaysia, and so on) can access the same international standard to calibrate the SBC solar input power. In addition, when used with sensible temperature measurements and calorimetric calculations a new range of solar cooking metrics becomes available.

For water-stressed communities' simple mass-based environmental factor (waste/product) calculations is used to help to minimize water usage. For solar cooked hard-boiled eggs-without water, eggs shell and carton result in a value close to 0.1, but never zero. However, the waste can be recycled without environmental harm. For the absorption method of cooking of White medium-grain rice, and rice-pudding, simple mass-based wastewater/product values are close to zero. Solar cooking of pastitsio #2 pasta, (like many other pasta types), require an excess of water, but through design water usage can be limited to approximately 0.6. Brown lentils however require an excess of water for cooking there have simple mass-based wastewater/product values of the order of 0.33 to 0.46.

In future work, Autodesk Revit® BIM software and SRA Insight plug-in (or other similar commercial software) modifications (geometry, and replacing solid

wood for transplant glass) to an existing SBC design may allow improvement in SBC solar energy input efficiency for winter months where low Sun slanting angles and shorter sunshine hours challenge efficient solar cooking. Such CAD simulations need to be revaluated in real-life using solar cooking metrics as presented here.

Conflicts of Interest

The authors declare no conflicts of interest regarding the publication of this paper.

References

[1] Kerr, B.P. (1991) The Expanding World of Solar Box Cookers. Barbara P. Kerr.

[2] Ciochetti, D.A. and Metcalf, R.H. (1984) Pasteurization of Naturally Contaminated Water with Solar Energy. *Applied and Environmental Microbiology*, **47**, 223-228. https://doi.org/10.1128/aem.47.2.223-228.1984

[3] Korená Hillayová, M., Holécy, J., Korísteková, K., Bakšová, M., Ostrihoň, M. and Škvarenina, J. (2023) Ongoing Climatic Change Increases the Risk of Wildfires. *Case Study: Carpathian Spruce Forests. Journal of Environmental Management*, **337**, Article 117620. https://doi.org/10.1016/j.jenvman.2023.117620

[4] NDC Partnership (2004) Solar Cookers How to Make, Use and Enjoy. 10th Edition. Solar Cookers International. https://www.solarcookers.org/files/7914/5687/8521/How_to_make_use_understand_English_Update.pdf

[5] Saxena, A., Goel, V. and Karakilcik, M. (2017) Solar Food Processing and Cooking Methodologies. In: *Energy, Environment, and Sustainability*, Springer, 251-294. https://doi.org/10.1007/978-981-10-7206-2_13

[6] Mendoza, J.M.F., Gallego-Schmid, A., Schmidt Rivera, X.C., Rieradevall, J. and Azapagic, A. (2019) Sustainability Assessment of Home-Made Solar Cookers for Use in Developed Countries. *Science of the Total Environment*, **648**, 184-196. https://doi.org/10.1016/j.scitotenv.2018.08.125

[7] Jaramillo, O.A., Huelsz, G., Hernández-Luna, G., del Río, J.A., Acosta, R. and Arriaga, L.G. (2007) Solar Oven for Intertropical Zones: Optogeometrical Design. *Energy Conversion and Management*, **48**, 2649-2656. https://doi.org/10.1016/j.enconman.2007.04.021

[8] Mudawia, H.A. and Ahmed, S.A. (2017) Comparative Study of Foods Cooked Using Solar Box & Butane Gas Cooker. *International Journal of Agriculture, Environment, and Bioresearch*, **2**, 494-504.

[9] Ambarita, H. (2018) Numerical Study on the Effect of Configuration of a Simple Box Solar Cooker for Boiling Water. *IOP Conference Series: Materials Science and Engineering*, **308**, Article 012028. https://doi.org/10.1088/1757-899x/308/1/012028

[10] Ademe, Z. and Hameer, S. (2018) Design, Construction and Performance Evaluation of Abox Type Solar Cooker with a Glazing Wiper Mechanism. *AIMS Energy*, **6**, 146-169. https://doi.org/10.3934/energy.2018.1.146

[11] Soe, N.N., Win, A.K. and Min, N.K.T. (2019) Design and Construction of Solar Box Cooker System. *IRE Journals*. **3**, 319-325.

[12] Anilkumar, B.C., Maniyeri, R. and Anish, S. (2020) Design, Fabrication and Performance Assessment of a Solar Cooker with Optimum Composition of Heat Storage Materials. *Environmental Science and Pollution Research*, **28**, 63629-63637.

https://doi.org/10.1007/s11356-020-11024-3

[13] Amosun, S.T., Samuel, O.D., Idi, S., Ashiedu, F.I., Fayomi, O.S.I., Anisiji, E.O., *et al.* (2021) Development and Performance Evaluation of a Box-Type Solar Cooker. *IOP Conference Series*: *Materials Science and Engineering*, **1107**, Article 012222. https://doi.org/10.1088/1757-899x/1107/1/012222

[14] Wassie, H.M., Getie, M.Z., Alem, M.S., Kotu, T.B. and Salehdress, Z.M. (2022) Experimental Investigation of the Effect of Reflectors on Thermal Performance of Box Type Solar Cooker. *Heliyon*, **8**, e12324. https://doi.org/10.1016/j.heliyon.2022.e12324

[15] Reasad, M., Islam, M.T. and Sumaiya, S. (2022) Development and Performance Analysis of a Box Type Solar Cooker Working on Low-Cost Thermal Energy Storage Material. *International Conference on Mechanical, Industrial and Materials Engineering* 2022, Bangladesh, 20-22 December 2022, Article ID: ICMIME2022_29.

[16] Vaidya, H., Rathod, M. and Channiwala, S. (2023) Design, Development, and Analysis of a Box Type Solar Cooker with Optimally Reflecting Side Walls. *Journal of Thermal Engineering*, **9**, 637-647. https://doi.org/10.18186/thermal.1297564

[17] Patel, A. (2023) Comparative Thermal Performance Analysis of Box Type and Hexagonal Solar Cooker. *International Journal of Sustainable Development Research*, **8**, 610-615.

[18] Adewole, B.Z., Popoola, O.T. and Asere, A.A. (2015) Thermal Performance of a Reflector Based Solar Box Cooker Implemented in Ile-Ife, Nigeria. *International Journal of Energy Engineering*, **5**, 95-101.

[19] Idriss, I.M. (2023) Performance Evaluation of Box-Type Solar Cookers Using Different Insulation Materials. *Nigerian Journal of Science and Engineering Infrastructure*, **1**, 19-30. https://doi.org/10.61352/2023at02

[20] Bhaumik, M., Sur, A. and Pasi, B. (2018) Design and Development of Economic and Portable Solar Cooker System Using Waste Materials. *Journal of Basic and Applied Research International*, **24**, 104-112.

[21] Manohar, K., Yearwoo, A., Lemessy, K. and Ramkissoon, K. (2023) Enhancing Solar Cooker Performance-Composite Design. *Conference Paper*: *International on Multidisciplinary Innovation in Academic Research* (*MIAR*-23), New York, December 2023, 54-60.

[22] Adetifa, B.O. and Aremu, A.K. (2016) Development and Evaluation of a Multi-Reflector Double Exposure Box-Type Solar Cooker. *Ife Journal of Technology*, **24**, 32-39.

[23] Folaranmi, J. (2013) Performance Evaluation of a Double-Glazed Box-Type Solar Oven with Reflector. *Journal of Renewable Energy*, **2013**, 1-8. https://doi.org/10.1155/2013/184352

[24] Soro, D., Soro, D., Sidibé, M., Doumbia, Y., Touré, S. and Marí, B. (2020) Theoretical and Experimental Studies of a Box-Type Solar Cooker in Unfavorable Climatic Conditions. *Smart Grid and Renewable Energy*, **11**, 51-60. https://doi.org/10.4236/sgre.2020.114004

[25] Milikias, E., Bekele, A. and Venkatachalam, C. (2020) Performance Investigation of Improved Box-Type Solar Cooker with Sensible Thermal Energy Storage. *International Journal of Sustainable Engineering*, **14**, 507-516. https://doi.org/10.1080/19397038.2020.1822456

[26] Milikias, E. and Alemayehub, A.B. (2023) Assessment of Solar Energy Potential for Solar Cooking—A Case of Daassenech, Ethiopia. *International Journal of Basic and Applied Research*, **5**, 164-181.

[27] Al-Nehari, H.A., Mohammed, M.A., Odhah, A.A., Al-attab, K.A., Mohammed, B.K.,

Al-Habari, A.M., *et al.* (2021) Experimental and Numerical Analysis of Tiltable Box-Type Solar Cooker with Tracking Mechanism. *Renewable Energy*, **180**, 954-965. https://doi.org/10.1016/j.renene.2021.08.125

[28] Terres, H., Lizardi, A., López, R., Vaca, M. and Chávez, S. (2014) Mathematical Model to Study Solar Cookers Box-Type with Internal Reflectors. *Energy Procedia*, **57**, 1583-1592. https://doi.org/10.1016/j.egypro.2014.10.150

[29] Terres, H., Chávez, S., Lizardi, A., Lara, A., Morales, J., Rodríguez, R., *et al.* (2022) Analysis of a Solar Cookers Box-Type with Inner Reflectors by Using CFD. *Journal of Physics*: *Conference Series*, **2307**, Article 012001. https://doi.org/10.1088/1742-6596/2307/1/012001

[30] Koshti, B., Dev, R., Bharti, A. and Narayan, A. (2023) Experimental Investigation and Performance Analysis of Box-Type Standard Solar Cooker with an Inclined Cover (BTSCIC). *Environmental Science and Pollution Research*, **30**, 117110-117131. https://doi.org/10.1007/s11356-023-30120-8

[31] Kesarwani, S., Rai, A.K. and Sachann, V. (2015) An Experimental Study on Box-Type Cooker. *International Journal of Advanced Research in Engineering and Technology*, **6**, 1-6.

[32] Srivastava, S.K. and Rai, A.K. (2023) Experimental Investigation on the Cooking the Cooking Vessel of Solar Box Cooker. *International Journal of Mechanical Engineering and Technology*, **1**, 62-69.

[33] Zafar, H.A., Khan, M.Y., Badar, A.W., Tariq, R. and Butt, F.S. (2018) Introducing a Novel Design in the Realm of Box Type Solar Cookers: An Experimental Study. *Journal of Renewable and Sustainable Energy*, **10**, Article 043707. https://doi.org/10.1063/1.5037981

[34] Ali Rizvi, S.A., Uzair, M. and Siddiqui, M.A. (2023) The Effects of Using Different Thermal Storage Materials and Their Mixtures on the Performance of a Solar Cooker. *Forschung im Ingenieurwesen*, **87**, 1285-1295. https://doi.org/10.1007/s10010-023-00714-2

[35] Mullick, S.C., Kandpal, T.C. and Saxena, A.K. (1987) Thermal Test Procedure for Box-Type Solar Cookers. *Solar Energy*, **39**, 353-360. https://doi.org/10.1016/s0038-092x(87)80021-x

[36] Sethi, V.P., Sumathy, K. and Pal, D.S. (2013) Optimum Inclination Angles of Booster Mirrors and Solar Radiation Availability on the Horizontal and Inclined Box Type Solar Cookers. *Journal of Power and Energy Engineering*, **1**, 53-57. https://doi.org/10.4236/jpee.2013.15008

[37] Poonia, S., Singh, A.K., Santra, P. and Jain, D. (2019) Development and Performance Evaluation of High Insulation Box Type Solar Cooker. *Agricultural Engineering Today*, **43**, 1-10. https://doi.org/10.52151/aet2019431.1490

[38] Nahar, N.M. (2003) Performance and Testing of a Hot Box Storage Solar Cooker. *Energy Conversion and Management*, **44**, 1323-1331. https://doi.org/10.1016/s0196-8904(02)00113-9

[39] Kalidasan, B., Chinnasamy, S., Pandey, A.K., Hassan, M.A. and Sharma, K. (2023) Thermal Performance Analysis of Solar Box Cookers Using Different Fin Configurations: An Experimental Investigation. *Journal of Thermal Analysis and Calorimetry*, **148**, 7421-7440. https://doi.org/10.1007/s10973-023-12236-8

[40] Kunene, N., Mhazo, N., Mukabwe, O. and Masarirambi, M.T. (2015) Fabrication and Testing of a Solar Cooker. *UNISWA Journal of Agriculture*, **18**, 49-59.

[41] Mawire, A., Lentswe, K., Owusu, P., Shobo, A., Darkwa, J., Calautit, J., *et al.* (2020)

Performance Comparison of Two Solar Cooking Storage Pots Combined with Wonderbag Slow Cookers for Off-Sunshine Cooking. *Solar Energy*, **208**, 1166-1180. https://doi.org/10.1016/j.solener.2020.08.053

[42] Benbaha, A., Yettou, F., Azoui, B., Gama, A., Rathore, N. and Panwar, N.L. (2024) Novel Mixed Solar Cooker: Experimental, Energy, Exergy, and Economic Analysis. *Heat Transfer*, **53**, 2095-2127. https://doi.org/10.1002/htj.23023

[43] Maammeur, H., Rouag, A., Belatrache, D., Bendaoud, B. and Moussaoui, Y. (2024) Experimental Investigation on Two Novel Standard Parameters to Improve the Performance of Solar Box Cookers. *Annals of West University of Timisoara—Physics*, **66**, 95-117. https://doi.org/10.2478/awutp-2024-0007

[44] Belatrache, D., Necib, H., Maammeur, H., Chaich, Z., Bougoffa, E. and Djeghab, A. (2024) Experimental Study of the Influence of Wing Reflectors on Solar Hot Box Cooker Performance. *International Journal of Environmental Science and Technology*, 1-14. https://doi.org/10.1007/s13762-024-05911-2

[45] Collares-Pereira, M., Cavaco, A. and Tavares, A. (2018) Figures of Merit and Their Relevance in the Context of a Standard Testing and Performance Comparison Methods for Solar Box—Cookers. *Solar Energy*, **166**, 21-27. https://doi.org/10.1016/j.solener.2018.03.040

[46] Arabacigil, B., Yuksel, N. and Avci, A. (2015) The Use of Paraffin Wax in a New Solar Cooker with Inner and Outer Reflectors. *Thermal Science*, **19**, 1663-1671. https://doi.org/10.2298/tsci121022031a

[47] Cuce, P.M., Kolayli, S. and Cuce, E. (2020) Enhanced Performance Figures of Solar Cookers through Latent Heat Storage and Low-Cost Booster Reflectors. *International Journal of Low-Carbon Technologies*, **15**, 427-433. https://doi.org/10.1093/ijlct/ctz079

[48] Qandil, A., Al-Younis, E.S., Saleh, A. and Hasson, M. (2018) Experimental Study of the Performance of a Box Solar Cooker. *International Journal of Scientific & Engineering Research*, **9**, 769-773.

[49] Kadhim, S.A. and Askar, A.H. (2018) Evaluation Performance of a Solar Box Cooker in Baghdad. *Journal of University of Babylon for Engineering Sciences*, **26**, 208-216.

[50] Ibrahim, O.A.A., Kadhim, S.A. and Ali, H.M. (2024) Enhancement the Solar Box Cooker Performance Using Steel Fibers. *Heat Transfer*, **53**, 1660-1684. https://doi.org/10.1002/htj.23008

[51] Kumar, A., Saxena, A., Pandey, S.D. and Joshi, S.K. (2022) Design and Performance Characteristics of a Solar Box Cooker with Phase Change Material: A Feasibility Study for Uttarakhand Region, India. *Applied Thermal Engineering*, **208**, Article 118196. https://doi.org/10.1016/j.applthermaleng.2022.118196

[52] Kumar, A., Saxena, A., Pandey, S.D. and Gupta, A. (2023) Cooking Performance Assessment of a Phase Change Material Integrated Hot Box Cooker. *Environmental Science and Pollution Research*, 1-16. https://doi.org/10.1007/s11356-023-25340-x

[53] Kambezidis, H.D. and Psiloglou, B.E. (2021) Estimation of the Optimum Energy Received by Solar Energy Flat-Plate Convertors in Greece Using Typical Meteorological Years. Part I: South-Oriented Tilt Angles. *Applied Sciences*, **11**, Article 1547. https://doi.org/10.3390/app11041547

[54] Darhmaoui, H. and Lahjouji, D. (2013) Latitude Based Model for Tilt Angle Optimization for Solar Collectors in the Mediterranean Region. *Energy Procedia*, **42**, 426-435. https://doi.org/10.1016/j.egypro.2013.11.043

[55] Chatelain, T., Mauree, D., Taylor, S., Bouvard, O., Fleury, J., Burnier, L., *et al.* (2019)

Solar Cooking Potential in Switzerland: Nodal Modelling and Optimization. *Solar Energy*, **194**, 788-803. https://doi.org/10.1016/j.solener.2019.10.071

[56] Kumaravel, A.R., Deenadayalan, N., Perumal, S.V. and Mohamed, A.A. (2024) Enhanced Solar Cooker with Automatic Sun Tracking and Vacuum Insulated Cooking Chamber. *International Journal of Electrical and Computer System Design*, **5**, 48-54.

[57] Cooper, P.I. (1969) The Absorption of Radiation in Solar Stills. *Solar Energy*, **12**, 333-346. https://doi.org/10.1016/0038-092x(69)90047-4

[58] Sheldon, R.A. (2023) The E Factor at 30: A Passion for Pollution Prevention. *Green Chemistry*, **25**, 1704-1728. https://doi.org/10.1039/d2gc04747k

[59] Wang, Y., He, X., Ouyang, F., He, J., Wu, W. and Wu, C. (2023) New Method for Fine Calculation of Bridge Temperature Field Based on BIM Solar Radiation Analysis. *Advances in Civil Engineering*, **2023**, 1-13. https://doi.org/10.1155/2023/6855116

[60] Perez, R., Stewart, R., Arbogast, C., Seals, R. and Scott, J. (1986) An Anisotropic Hourly Diffuse Radiation Model for Sloping Surfaces: Description, Performance Validation, Site Dependency Evaluation. *Solar Energy*, **36**, 481-497. https://doi.org/10.1016/0038-092x(86)90013-7

[61] Law, V.J. and Dowling, D.P. (2018) Converting a Microwave Oven into a Plasma Reactor: A Review. *International Journal of Chemical Engineering*, **2018**, 1-12. https://doi.org/10.1155/2018/2957194

[62] Law, V.J. and Dowling, D.P. (2023) Revisiting "Non-Thermal" Batch Microwave Oven Inactivation of Microorganisms. *American Journal of Analytical Chemistry*, **14**, 28-54. https://doi.org/10.4236/ajac.2023.141003

[63] Baig, M.M., Khan, M.A., Uddin, M.K.M. and Malik, M.R. (2017) Calculation and Fabrication of a Solar Flat Plate Collector Efficiency Using Mild Steel as Absorber Plate. *International Journal of Science Technology & Engineering*, **3**, 36-41.

[64] Coimbra, J.S.R., Gabas, A.L., Minim, L.A., Garcia Rojas, E.E., Telis, V.R.N. and Telis-Romero, J. (2006) Density, Heat Capacity and Thermal Conductivity of Liquid Egg Products. *Journal of Food Engineering*, **74**, 186-190. https://doi.org/10.1016/j.jfoodeng.2005.01.043

[65] Munir, M.T., Zhang, Y., Yu, W., Wilson, D.I. and Young, B.R. (2016) Virtual Milk for Modelling and Simulation of Dairy Processes. *Journal of Dairy Science*, **99**, 3380-3395. https://doi.org/10.3168/jds.2015-10449

[66] Law, V.J. (2024) Mass-Based Environmental Factor and Energy Assessment of Microwave-Assisted Synthesized Transition Metal Nanostructures. *American Journal of Analytical Chemistry*, **15**, 201-218. https://doi.org/10.4236/ajac.2024.156013

[67] Anilkumar, B.C., Maniyeri, R. and Anish, S. (2021) Numerical Investigation on the Effect of Various Geometries in a Solar Box-Type Cooker: A Comparative Study. In: *Lecture Notes in Mechanical Engineering*, Springer, 81-89. https://doi.org/10.1007/978-981-16-0698-4_9

[68] https://www.scienceofcooking.com/eggs/cooking-eggs-sous-vide.html

[69] https://www.youtube.com/watch?v=1cE0geJY1SI

[70] Hwang, J., Ha, J., Siu, R., Kim, Y.S. and Tawfick, S. (2022) Swelling, Softening, and Elastocapillary Adhesion of Cooked Pasta. *Physics of Fluids*, **34**, Article 042105. https://doi.org/10.1063/5.0083696

[71] Martins, G.N., Carboni, A.D., Hugo, A.A., Castilho, P.C. and Gómez-Zavaglia, A. (2023) Chickpeas' and Lentils' Soaking and Cooking Wastewaters Repurposed for

Growing Lactic Acid Bacteria. *Foods*, **12**, Article 2324. https://doi.org/10.3390/foods12122324

[72] Fernandez-Burgos, M., Tracy-Wanck, S., *et al.* (2008) Solar Cooker Earth Analog and Comparison of Design Efficacy. Spring 2008-Global Climate Change EES 359.

[73] Law, V.J. and Dowling, D.P. (2023) Green Chemistry Allometry Test of Microwave-Assisted Synthesis of Transition Metal Nanostructures. *American Journal of Analytical Chemistry*, **14**, 493-518. https://doi.org/10.4236/ajac.2023.1411029

[74] Zhai, Y., Yang, J., Zhu, Y., Du, Q., Yuan, W. and Lu, H. (2020) Quality Change Mechanism and Drinking Safety of Repeatedly-Boiled Water and Prolonged-Boil Water: A Comparative Study. *Journal of Water and Health*, **18**, 631-653. https://doi.org/10.2166/wh.2020.022